ISSN 1063-7834, Physics of the Solid State, 2019, Vol. 61, No. 12, pp. 2254–2259. © Pleiades Publishing, Ltd., 2019.
Russian Text © The Author(s), 2019, published in Fizika Tverdogo Tela, 2019, Vol. 61, No. 12, pp. 2274–2279.

METALS

Degenerate Structure of Transformation Twins and Estimation of Dislocation Density in Martensite Crystals

M. P. Kashchenko[a, b, *], N. M. Kashchenko[a], and V. G. Chashchina[a, b]

[a] *Ural Federal University Named after the First President of Russia B.N. Yeltsin, Yekaterinburg, Russia*

[b] *Ural State Forest Engineering University, Yekaterinburg, Russia*

**e-mail: mpk46@mail.ru*

Received July 16, 2019; revised July 16, 2019; accepted July 25, 2019

Abstract—In the dynamic theory of martensitic transformations, the wave mechanism of controlling martensite crystal growth is determined by the superposition of wave beams of quasi-longitudinal (or longitudinal) waves carrying the "tensile–compression" deformation in the orthogonal directions. The wave beam formation is considered to be a result of the formation of excited (vibrational) states. The existence of transformation twins is interpreted as a result of a matched propagation with respect to long-wave (*l* waves) and short-wave (*s* waves) shifts. The matching condition is analyzed for the γ–α martensitic transformation in iron-base alloys. It is shown for the first time that the transition to a degenerate twin structure with the allowance for the medium discreteness enables one to estimate the dislocation density in crystals with habit {557}, which agrees with that observed experimentally.

Keywords: martensitic transformations, transformation twins, controlling wave process, habit planes, degenerate twin structure, dislocation density

DOI: 10.1134/S1063783419120187

1. INTRODUCTION

Martensitic transformations (MT) are observed in many crystalline materials; they have a cooperative character and occur, as a rule, with marks of a first-order phase transition. The attempts of interpretation of a heterogeneous nucleation based on traditional concepts of the existence quasi-equilibrium nuclei of a new phase, on the one hand, are not strengthened by reliable observations of similar nuclei (the problem of unobservability of nuclei), and, on the other hand, do not enable adequate interpretation of an abundant set of the MT features observed experimentally.

These problems are particularly clearly observed in the attempts of describing the fcc–bcc (bct) transformation in iron alloys. The study of this transformation (for shortness, γ–α MT) favored to storage of the most information laid in the base of definition of the martensitic transformation as a specific (diffusion-less) cooperative transformation [1]. The most clear feature of a spontaneous (on cooling) γ–α MT is the supersonic (with respect to longitudinal waves) growth rate of martensite crystals. This circumstance immediately enables us to exclude from consideration dislocation models of crystal growth, unambiguously indicating the wave nature of controlling crystal growth. This, it should be to reveal the specific features of the heterogeneous start of the crystal growth, which leads to the appearance of a wave process controlling crystal formation and allowing us to interpret the observed set of morphological indicators. This program was performed during developing the dynamic MT theory [2–4].

In this case, the concept of the initial excited (vibrational) state (IES) plays a central part. IES appears in elastic fields of individual dislocations; it has a shape of an elongated parallelepiped with the edge orientations close to the orientations of eigenvectors ξ_1, ξ_2, and ξ_3 of the elastic field deformation tensor of the dislocation nucleation center (DNC). In this case, in the region favorable for appearance of IES, two eigenvalues of the deformation tensor have opposite signs, and the third deformation is small ($\varepsilon_1 > 0$, $\varepsilon_2 < 0$, $\varepsilon_3 \ll |\varepsilon_{1,2}|$). The absolute values $|\varepsilon_{1,2}|$ are assumed to be comparable with the threshold values of the interphase barriers $\varepsilon_{th} \sim 10^{-4}$–$10^{-3}$. Then on cooling to temperature M_s (below the temperature of phase equilibrium T_0), in the region with a decreased value of the threshold deformation, IES appears stepwise with a matched fast jump of atoms to new equilibrium positions with the excitation of vibrations in the orthogonal directions close to ξ_1 and ξ_2. Similar vibrations generate wave beams with the orthogonal wave vectors and velocities $\mathbf{v}_1$ and $\mathbf{v}_2$. In this case, the substantial region of superposing the wave beams, in which the threshold deformation takes place, is of the "tensile–compression" type (Fig. 1).

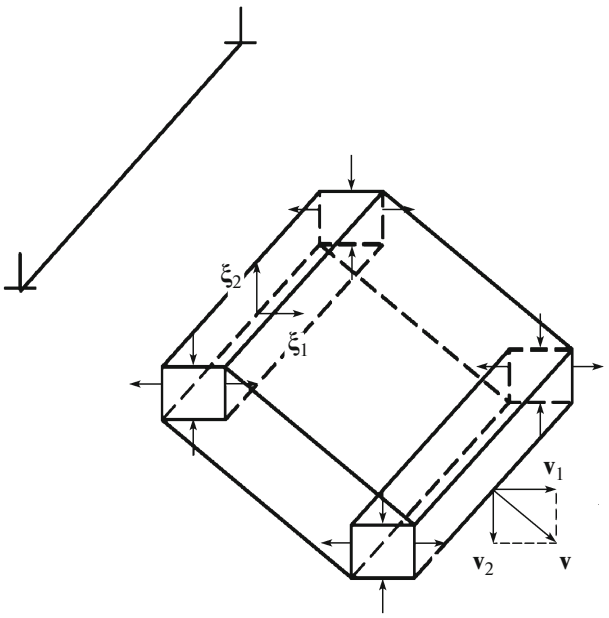

Fig. 1. Two-wave scheme of formation of a lamellar martensite crystal [3].

As follows from Fig. 1, in this model, the plane crystal boundaries (interphase boundaries–habits) correspond to the motion of the front intersection line of the wave beams at a velocity $\mathbf{v} = \mathbf{v}_1 + \mathbf{v}_2$. Thus, the formation of IEC gives rise to the simplest variant of controlling wave process (CWP). Below we will call this pair of quasi-longitudinal waves with relatively large wavelengths *l*-waves. It is easy to see that the orientation of normal **N** to the habit plane is given by relationship

$$\mathbf{N}_{1,2l} \parallel \mathbf{n}_{2l} \pm \kappa_{ll}\mathbf{n}_{1l}, \quad \kappa_{ll} = \frac{v_{2l}}{v_{1l}}, \quad |\mathbf{n}_{1,2l}| = 1,$$
$$\mathbf{n}_{1l} = \frac{\mathbf{v}_{1l}}{v_{1l}}, \quad \mathbf{n}_{2l} = \frac{\mathbf{v}_{2l}}{v_{2l}}. \tag{1}$$

However, martensite crystals can also exhibit a fine structure of transformation twins. The transformation twins form immediately during growing martensite crystals as alternating lamellar components. They are observed as in the case of pronounced markers of the first-order phase transitions (for example, in iron alloys [1]), so at MTs close to the second-order phase transitions (for example, in a number of nonferrous-metal alloys [5]). The typical difference of the twin structure component is the difference of the orientations of principal axes of strain, which are, as a rule, orthogonal to one another in the initial phase.

At comparatively low (subsonic) growth rates of martensite crystals, the dislocations concepts can be used as a growth mechanism when interpreting twin systems (e.g., [6]). However, at high growth rates of crystals with twin structures, it is natural to use dynamic (wave) interpretations based on the CWP concept. In preceding works, it was shown that the CWP concept, in which shorter *s*-waves are included to the CWP structure, makes it possible to describe not only the ideal (strictly regular) twin structure [3, 7, 8], but also to formulate and resolve the problem of interpretation of real inhomogeneous TS variants, based on the model of formation of a regular TS [9–13]. A principal result of this analysis is the conclusion on the TS fragmentation, in which each fragment is generated by the only excited cell formed spontaneously and initiating *s*-waves. The dynamic theory enables us to consider also the limiting case of a degenerate twin structure (DTS), in which the main component dominates [14].

It is well known [1] that, among the morphological types observed at γ–α MTs in iron allows, two crystal variants with habits close to {225} and {259}–{31015} (the crystallographic denotations are given in the initial γ-phase basis) have partially or completely twinned central part. Conversely, the crystals with habits close to the {557} family do not have similar twin structure, but demonstrate a high dislocation density in martensite. Thus, the question of what are the reasons of this difference rose regularly. The purpose of this work is to show that the transition to the degenerate twin system can be accompanied by the formation of dislocations and to estimate the dislocation density, using crystals with habits close to {557} as an example.

2. MAIN CONCEPTS OF FORMATION OF TWIN AND DEGENERATE TWIN STRUCTURES

Recall that, at γ–α MTs, the transformation twins contact by planes {110}. Such planes give pairs of *s*-waves propagating along orthogonal axes ⟨100⟩ and ⟨010⟩ of the initial phase (directions of Δ in the first Brillouin zone) at velocities $v_{s\Delta}$. Actually, the orientations of normals

$$\mathbf{N}_{1,2,s} \parallel [110], [1\,\bar{1}0] \tag{2}$$

to twinning planes are trivially found from Eq. (1) at the substitutions

$$\kappa_{ll} \to \kappa_{ss} = 1, \quad \mathbf{n}_{1l} \to \mathbf{n}_{1s} = [010],$$
$$\mathbf{n}_{2l} \to \mathbf{n}_{2s} = [100]. \tag{3}$$

The splitting mechanism on the orientations of the twinning planes was considered in detail in [3]. If the formation of IES initiating *l* waves is accompanied by more or less synchronized formation, in the region of IES localization, also the excited region in the shape of a thin vibrating parallelepiped, which initiates the excitation of pairs of *s* waves, the resulting controlling wave process enables a correct description of the formation of thin-plate twin crystals (or twinned central regions of lens-shaped crystals). In this case, the main TS components are physically separated, since it is

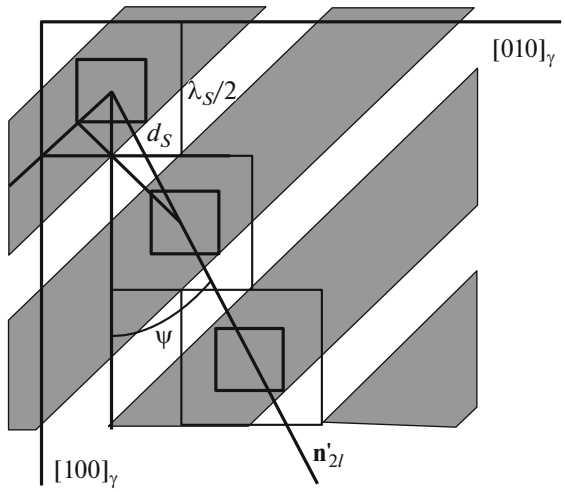

Fig. 2. Dynamic model of formation of a regular layered structure with ratio of component fractions 2/1 [12].

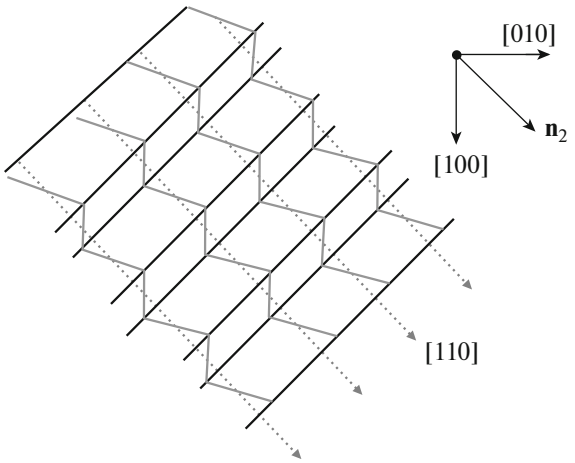

Fig. 3. System of alternating shifts in the main and additional components of the regular layered structure at the ratio of component volumes 2/1 [3].

precisely they are initiated by the action of waves, but twin interlayers form due to the coherent bond of contacting lattice regions.

The process of induced reproduction of the excited *s* cell is realized after passing, for the same time, two triangle legs by the superposition of *s* waves in directions [1 $\bar{1}$0] and [110] and the triangle hypotenuse by *l* wave carrying the compressive deformation at a velocity equal to projection v'_{2l} of velocity v_{2l} on the (001) plane (Fig. 2). At the velocity of passing of the triangle legs equal to $\sqrt{2}v_{s\Delta}$, we obtain condition

$$v_{s\Delta} = v'_{2l}\cos\psi, \tag{4}$$

where ψ is the acute angle between n'_{2l} and $v_{s\Delta} \parallel \langle 001\rangle_\gamma$. The harmonic description of the threshold deformation suggests that the initial phase lattice losses its stability in the region with transverse size $d_s < \lambda_s/2$, where λ_s is the *s*-wave length. Then, we find for ratio β_{tw} of the TS component volumes

$$\beta_{tw} = 4\tilde{d}_s/(1 + \tan\psi - 4\tilde{d}_s), \quad \tilde{d}_s = d_s/\lambda_s < 1/2. \tag{5}$$

According to Eq. (5), the case of the degenerate twin structure corresponds to the fulfillment of condition

$$1 + \tan\psi - 4\tilde{d}_s = 0. \tag{6}$$

This variant that leads to singularity $\beta_{tw} \to \infty$ is related to a continual description, which does not take into account the crystal medium discreteness. The coherence of conjugating the components, as is clear from Fig. 3, demonstrates the possibility of removing the singularity by generation of a dislocation at the place of the twin interlayer.

Actually the minimum thickness of the layer between the main TS components is the distance between the nearest atomic planes (110), i.e., $a/\sqrt{2}$, where *a* is the fcc-lattice parameter. If the relative shift of the neighboring planes will have the same value, which corresponds to the Burgers vector of perfect dislocation, it is reasonable to expect the generation of a dislocation loop, the main segments of which have a screw orientation. It is clear that, in this case, the shear deformation in the twin component is $\tan\varphi_{tw} = 1$. Since the twin component is in framing of the pair of the main TS components, each of the main components makes contribution $a/2\sqrt{2}$ to the relative shift of the neighboring planes. This was shown in [3]. During twinning, the first fast stage of the deformation is related to the action of *s* waves and, in the case of the equality of the velocities, we should also expect the equality of the values of the compressive and tensile strains: $\varepsilon_{1s} = |\varepsilon_{2s}| = \varepsilon_s$. The equality refers not only to threshold ε_{sth}, but also to the finish values of the first stage strain ε_{sf}.

This implies that the resulting shear strain in the main TS component with thickness $d_s\sqrt{2}$ is $\tan\varphi_{bas} = \varepsilon_{sf}$. It follows that the dislocation generation is possible even at the first deformation stage as the condition

$$d_s\sqrt{2}\varepsilon_{sf} = a/2\sqrt{2}, \quad d_s\varepsilon_{sf} = a/4 \tag{7}$$

is fulfilled.

Recall [3]: in the case as a twin component forms actually, it is reliable to suggest that the Bain-type compression deformation ($|\varepsilon_{2B}| \le 0.2$) in the twin region is attained already at the first deformation stage, while only a smaller tensile deformation can be attained in the main component. In the case with degenerate twin structure, instead of the twin martensite interlayer in layered structure directed by the controlling wave process, dislocations are generated,

which requires strains ε_{sf}, which are slightly lower, but of the same order, than $|\varepsilon_{2B}|$. The refinement of the value of ε_{sf} is possible, if we take into account that, according to Eq. (5), the maximum value of $d_{s\max} = \lambda_s/2$. Therefore, the determination of the value λ_s from the additional condition would allow us also to find the value ε_{sf} using Eq. (7). Such an additional condition is relationship (4) for the velocities of *s* and *l* waves.

3. FULFILLMENT OF THE CONDITION OF MATCHING VELOCITIES OF *s*- AND *l*-WAVES AND THE ESTIMATION OF THE DISLOCATION DENSITY

Note that, in the cases of twinning in crystals with habits (3 10 15)–(259), condition (4) optimal for the formation of a regular TS is not exactly fulfilled at the observed elastic moduli. Moreover, it cannot be also fulfilled due to the inclusion of a dispersion, which decreases $v_{s\Delta}$ at the quasi-momentum increases. Actually, according to the Christoffel equation [15], in the cubic lattice symmetry plane (001), in an arbitrary direction [cosψ, sinψ, 0] that form angle ψ with axis [100], in the long-wave limit, the ratio of the longitudinal wave velocities is determined by relationship

$$\frac{v(\psi)}{v_\Delta} = \sqrt{1 + \left(\frac{C_L}{C_{11}} - 1\right)(\sin 2\psi)^2}, \quad (8)$$

where C_L and C_{11} are elastic moduli given the longitudinal wave velocities in the directions of the second-order (v_Σ) and forth-order (v_Δ) symmetry axes. It is easy to assure that, substituting the values of the measured elastic moduli [16] in Eq. (8) at comparatively low angles, we have

$$\frac{v(\psi)}{v_\Delta} > \frac{1}{\cos(\psi)}. \quad (9)$$

For crystals with habits close to $\{31015\}_\gamma$–$\{259\}_\gamma$, angle ψ is varied from ~16.7° to ~21.8°, and inequality (9) is fulfilled and becomes stronger in going to $v_s < v_\Delta$. Because of this we do not observe regular twin structures. Conversely, as ψ tends to π/4, we have

$$\frac{v(\psi)}{v_\Delta} < \frac{1}{\cos(\psi)}. \quad (10)$$

Therefore, a decrease in velocity v_Δ in going to $v_s < v_\Delta$ will lead to equality (4).

It is pertinent to note that, in the dynamic theory, the existence of habits {557} is easily explained [2] (including also a small difference in the values of the pair of indices) as a result of propagating pairs of *l* waves near the pairs of the orthogonal directions ⟨110⟩ and ⟨001⟩, but the possibility of including *s* waves in the CWP composition for this case was not taken into account before. Since the angle between ⟨110⟩ and ⟨101⟩ is π/4, the description of crystals with habits {557} in the case of a degenerate twin structure, is actually related with the requirement

$$v_{s\Delta} = v'_{2l}\cos\pi/4 \approx v_\Sigma/\sqrt{2}. \quad (11)$$

Now we find the *s*-wave quasi-momentum, at which requirement (11) obeys. To do this, we use the analytical interpolation of the phonon dispersion law ε_k in the Δ direction [10], which is matched well with the sound velocity measurements [16] and with the neutron diffraction data [17]. The dispersion law ε_k along $\langle 001\rangle_\gamma$ for $0 \le k \le k_{\max} = 2\pi/a$ (*a* is the lattice parameter) is approximated in dimensionless variables *y* and *x* by function

$$1 - y = (1 - x)^p, \quad y = \varepsilon_k/(\varepsilon_k)_{\max}, \quad x = k/k_{\max}. \quad (12)$$

For example, for the Fe30Ni alloy the fcc lattice, the agreement with the experimental data is attained at $p \approx 1.733$. For group velocities $v_g(x) = dy/dx$ of *s*-waves, we have

$$v_{sg}(x) = dy/dx = p(1-x)^{p-1}, \quad v_g(0) = v_\Delta = p,$$
$$v_{sg}(x)/v_g(0) = v_{sg}(x)/p = (1-x)^{p-1}. \quad (13)$$

Actually, we are interested in ratio

$$v_{sg}(x)/v_\Sigma = (v_{sg}(x)/v_\Delta)(v_\Delta/v_\Sigma) = (1-x)^{p-1}\sqrt{\frac{C_{11}}{C_L}}. \quad (14)$$

Substituting $C_{11} = 0.1745$ TPa and $C_L = 0.2508$ TPa, according to the data of [16] for Fe-31.5 at a temperature of 673 K, in Eq. (14) and requiring

$$v_{sg}(x)/v_\Sigma = (1-x)^{p-1}\sqrt{\frac{C_{11}}{C_L}} = \frac{1}{\sqrt{2}}, \quad (15)$$

we find, at $p = 1.733$, that $x \approx 0.2$, i.e. $q_s \approx 0.2q_{\max} = 0.4\pi/a$. Therefore, $d_{s\max} = \lambda_s/2 = 2.5a$.

Then, from Eq. (7), we obtain $\varepsilon_{sf} = 0.1$. Thus, at the first stage, the *s*-strain is the value $\varepsilon_s = 0.1$. Let us assume that only one dislocation loop is generated in the interlayer between the neighboring main components of the degenerate twin structure, giving a pair of lines in the cross-section. From the geometry of nucleation of a lath crystal, it follows that these lines are directed along the elongated axis of the initial excited state, i.e., at habit (557) along $[1\,\bar{1}0]$. This variant is demonstrated in Fig. 4.

Then, for dislocation density ρ, we have

$$\rho \approx 2/(2d_s/d) = 1/(d_s/d). \quad (16)$$

At crystal thickness $d = 1$ μm $= 10^{-4}$ cm, $d_s = 2.3a$, and $a \approx 3.5 \times 10^{-8}$ cm, we obtain the estimation $\rho \approx 1.14 \times 10^{11}$ cm^{-2}, which correlates with the experimental data [1, 18, 19].

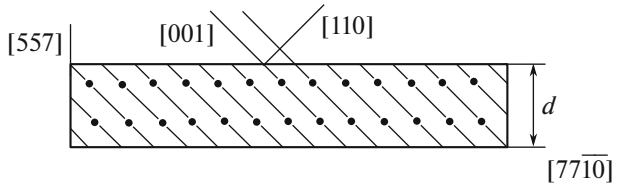

Fig. 4. Scheme of the intersection of a crystal with a degenerate twin structure with habit {557} by plane $(1\,\bar{1}0)$: the pair of points in lines [001] are the traces of the main segments of dislocation loops in planes (110) with the screw orientation of the Burgers vector; the distance between the planes of the neighboring loops is $d_s\sqrt{2}$.

4. DISCUSSION

First, we note that the crystals with the habits close to {557} have the shape of "laths." i.e., they are clearly nonequiaxial crystals. The ensembles of such crystals form specific colonies called "packets" (the crystals in each packet can contain no more than six variants from 24 possible variants [19]). Thus, it is interesting to explain the features of the formation of both an individual crystal and the whole ensemble of packet martensite. From positions of minimizing elastic energy, the qualitative interpretation reduces to that the crystal grouping into packets reflect the variant of accommodating internal stresses.

In addition, crystals with habits {557} form at relatively high temperatures, and the relaxation of induced stresses is performed by shears into the surrounding retained austenite. However, this fact does not explain high dislocation density inside martensite.

In the dynamic theory, the features of the formation of a packet of crystals is naturally interpreted as a self-organization process of wave growth of individual crystals in elastic fields of the dislocation nucleation center, the sequential formation of which is initiated by growing crystals [20, 21]. It was already noted above that the existence of habits {557} is a result of a propagation of pairs of *l* waves near orthogonal directions ⟨110⟩ and ⟨001⟩. Since the Bain-type deformation is three-dimensional, it was assumed, without consideration of *s* waves in the composition of the controlling wave process, that the deformation in the third orthogonal direction is performed due to the electron correlations, which restores the electron density symmetry. In [21], the formation of the observed dislocation density is related to the processes of propagating and partial annihilation of crystons, which are the volume carriers of the shear deformation of the superdislocation type.

The variant of [22] that interpret the formation of crystals as a process of deformation of the {110} planes is also of interest. However, we assume that the interpretation of the dislocation formation as a result of developing degenerate twin structure in conditions of matching the *s*-wave and *l*-wave deformations proposed in this work is the most preferential. Actually, this MT mechanism immediately provides a three-dimensional deformation, removing the indeterminacy when choosing the orientation of the principal contraction axis leading to the rule, which is general for habits {*hkl*}. Namely: at $|h| < |k| < |l|$, the principal axis orientation is correlated to direction ⟨010⟩ with the position of units corresponding to the position of the middle index *k* in the habit recording. The position of the largest index 1 is correlated with the tensile direction ⟨001⟩. Recall that the recording of habit {557} with the equality of the pair of indices is justified if both the *l*-waves lie in the $\{1\,\bar{1}0\}$ plane. This variant is possible as the initial excited state forms in elastic fields of edge dislocations with lines $\langle 1\,\bar{1}0\rangle$. However, in the case of 60-deg dislocations, the appearance of the initial excited state leads to the exit of the wave vector of the *l*-wave that carries the compressive deformation from plane $\{1\,\bar{1}0\}$. This leads to the deviation of $\mathbf{n}_{2l}$ on direction ⟨110⟩ in plane {001} and, correspondingly, to the violation of the equality of the pair of indices, the difference of ψ from $\pi/4$ and to the choice of the same axis of axes ⟨100⟩ or ⟨010⟩, which makes a smaller angle with $\mathbf{n}_{2l}$ as the principal axis of contraction. It is clear that, at $\psi < \pi/4$, it is the ⟨100⟩ axis. In addition, at $\psi < \pi/4$, the inequality $d_s < \pi/4$ and, therefore, a nonzero threshold deformation, corresponds to condition (6) for the transition to the degenerate twin system. It is clear that, at $\psi < \pi/4$, the inequality $d_s < \lambda_s/2$, i.e., a nonzero threshold deformation, corresponds to condition (6) for the transition to the degenerate twin system.

We also note that the absence of transformation twins in lath crystals was considered before as a result of high damping of *s* waves. However, the transparent interpretation of the dislocation nucleation mechanism based on the efficiency of the short-wave shifts indicates that their lifetime is sufficient for realization of MT. This fact is likely due to the supporting *s* waves by a nonequilibrium electron subsystem [2, 4, 23]. It is clear that the deviations from the fulfillment of condition (4) at the spontaneous formation of active *s*–*l* cells generating *s* waves are inevitable. A decrease in the *s*-wave quasi-momenta will be accompanied by an increase in λ_s and d_s and, therefore, according to Eq. (17), a decrease in the dislocation density. Conversely, a decrease in thicknesses *d* leads to an increase in density ρ. Thus, it should be expected that, in the crystal packets, ρ have values 10^{10}–10^{12} cm^{-2}.

5. CONCLUSIONS

The dynamic theory of formation of regular layered structures during MTs, including the transformation twins makes it possible to perform the limiting transition to a degenerate structure, taking into account the discreteness of the crystal medium.

It is shown that, in the case of the formation of crystals with habits {557}, the condition of matching for the velocities of short-wave and long-wave shifts, which enables the introduction of a regular structure, in which dislocation loops form instead of twin interlayers, is fulfilled. The estimation of the dislocation density performed in this model agrees with the values observed experimentally.

ACKNOWLEDGMENTS

The authors are grateful to participants of the XXI Winter School on the Mechanics of Continua (Perm, February 18–22, 2019) and the International Conference MGCTF-2019 (St. Petersburg, July 1–5, 2019) for discussion of the results.

CONFLICT OF INTEREST

The authors declare that they have no conflicts of interest.

REFERENCES

1. G. V. Kurdyumov, L. M. Utevskii, and R. I. Entin, *Transformations in Iron and Steel* (Nauka, Moscow, 1977) [in Russian].
2. M. P. Kashchenko, *The Wave Model of Martensite Growth in the Case of γ–α Transformations in Iron-Based Alloys*, 2nd ed. (Regul. Khaotich. Dinam., Moscow, Izhevsk, 2010) [in Russian].
3. M. P. Kashchenko and V. G. Chashchina, *A Dynamic Model of the Formation of Twin Martensitic Crystals at γ–α Transformations in Iron-Based Alloys* (Ural. Gos. Lesotekh. Univ., Yekaterinburg, 2009) [in Russian].
4. M. P. Kashchenko and V. G. Chashchina, Phys. Usp. **54**, 331 (2011).
5. H. Warlimont and L. Delay, *Martersitic Transformations in Copper-, Silver- and Gold-Based Alloys* (Pergamon, Oxford, 1974).
6. M. A. Shtremel', *The Strength of Alloys. Part. 2: Deformation* (MISIS, Moscow, 1997) [in Russian].
7. M. P. Kashchenko, V. G. Chashchina, and S. V. Vikharev, Phys. Met. Metallogr. **110**, 200 (2010).
8. M. P. Kashchenko, V. G. Chashchina, and S. V. Vikharev, Phys. Met. Metallogr. **110**, 305 (2010).
9. M. P. Kashchenko and V. G. Chashchina, Phys. Met. Metallogr. **114**, 821 (2013).
10. M. P. Kashchenko, I. F. Latypov, and V. G. Chashchina, Lett. Mater. **7**, 146 (2017).
11. M. P. Kashchenko and V. G. Chashchina, Phys. Met. Metallogr. **118**, 311 (2017).
12. M. P. Kashchenko, N. M. Kashchenko, and V. G. Chashchina, Mater. Today **4**, 4605 (2017).
13. M. P. Kashchenko, N. M. Kashchenko, and V. G. Chashchina, Phys. Met. Metallogr. **119**, 1 (2018).
14. M. P. Kashchenko, N. M. Kashchenko, and V. G. Chashchina, Lett. Mater. **8**, 429 (2018).
15. F. I. Fedorov, *Theory of Elastic Waves in Crystals* (Nauka, Moscow, 1965) [in Russian].
16. G. Haush and H. Warlimont, Acta Met. **21**, 400 (1973).
17. E. D. Hallman and B. N. Brockhouse, Can. J. Phys. **47**, 1117 (1969).
18. T. V. Eterashvili, L. M. Utevskii, and M. N. Spasskii, Fiz. Met. Metalloved. **49**, 807 (1979).
19. D. P. Rodionov and V. M. Schastlivtsev, *Steel Single Crystals* (UrO RAN, Yekaterinburg, 1996) [in Russian].
20. V. P. Vereshchagin, M. P. Kashchenko, S. V. Konovalov, and T. N. Yablonskaya, Fiz. Met. Metalloved. **77**, 173 (1994).
21. M. P. Kashchenko, V. V. Letuchev, S. V. Konovalov, and T. N. Yablonskaya, Phys. Met. Metallogr. **83**, 237 (1997).
22. V. G. Chashchina, Russ. Phys. J. **52**, 766 (2009).
23. M. P. Kashchenko, N. A. Skorikova, and V. G. Chashchina, Phys. Met. Metallogr. **106**, 219 (2008).

Translated by Yu. Ryzhkov